Scientific Research Publishing

Advances in Aerospace Science and Technology, 2021, 6, 114-121
https://www.scirp.org/journal/aast
ISSN Online: 2473-6724
ISSN Print: 2473-6708

# A Study of the Deformation Derivatives for a Ti-6Al-4V Inertia Friction Weld

**Richard P. Turner*, Nils Warnken, Jeffery W. Brooks**

School of Metallurgy & Materials, University of Birmingham, Birmingham, UK
Email: *r.p.turner@bham.ac.uk

**How to cite this paper:** Turner, R.P., Warnken, N. and Brooks, J.W. (2021) A Study of the Deformation Derivatives for a Ti-6Al-4V Inertia Friction Weld. *Advances in Aerospace Science and Technology*, **6**, 114-121.
https://doi.org/10.4236/aast.2021.62008

**Received:** April 13, 2021
**Accepted:** June 6, 2021
**Published:** June 9, 2021



## Abstract

The velocity–versus-time rundown curves from two experimental Ti-6Al-4V inertia friction welds were analysed and differentiated several times, to produce rotational acceleration, jerk, jounce (or snap), crackle and pop versus-times curves for each weld. Titanium alloys and their mechanical properties are known to be highly sensitive to strain rate as the material is deformed, though nothing has ever been considered in terms of the higher-order time-derivatives of position. These curves have been studied and analysed further, for a more complete understanding of the derivative trends. Rotational acceleration and jerk traces both display behavior patterns across the two welds as the part rotates under action from the flywheel. The rotational snap also displays a pattern in this derivative during the final approximately 0.5 s of welding, as the energy dissipates. Evidence of a distinct oscillatory pattern in the rotational crackle and pop terms was noted for one weld when differentiating over a larger time-base, though could not be replicated in the 2nd weld. The higher derivative curves allow distinction of different process regimes, indicating that inertial energy mostly influences the time-base of dynamically steady-state phase. Qualitative differences between initial energies are evident in higher derivatives.

## Keywords

Rotation, Acceleration, Jerk, Snap, Crackle, Pop

## 1. Introduction

Inertia friction welding (IFW) is the most commonly used friction joining process [1], and a much-used manufacturing method within aerospace [2], automotive [3] and power generation industries. During an IFW process, one axisymmetric component is held, whilst another is attached to a flywheel and rotated under the

stored energy of the flywheel [4]. The titanium alloy Ti-6Al-4V is commonly used in the aerospace and aeroengine industries, primarily thanks to its excellent strength-to-weight ratio. As such, Ti-6Al-4V is one of the more commonly studied materials within IFW processing [4] [5]. Three distinct phases are commonly identified during the weld process [5]. Firstly, the conditioning phase sees the components heated at the faying interface by frictional mechanisms. Secondly, the equilibrium or burn-off phase sees the process force the sacrificial interface material out of the joint, and into the formed flash. Lastly, once the flywheel has exhausted its stored energy, a forging phase consolidates the welding with a small further amount of axial shortening [6].

As such, the process is a highly dynamic manufacturing operation, with the component undergoing rapid rotational displacement caused by the dissipating energy from the flywheel. This rapidly changing energy yields constantly evolving rotational velocity, and as such evolving rotational acceleration, rotational jerk, and higher time-derivatives of rotational position. Whilst the rotational velocity, often referred to as the "run-down", is analysed by manufacturing engineers to understand more about the process, the higher derivatives are not. Titanium alloys display mechanical property sensitivity to the microstructure and grain size, as well as strain-rate sensitivity [7]. The yield strength of these flow stress curves increases significantly, with the higher strain-rates observed close to the weld line during processing.

However, little work has been considered regarding any potential 2$^{nd}$, 3$^{rd}$ or higher-order derivative of deformation and in turn any potential material property sensitivity. It, therefore, remains largely unconsidered and unknown how these properties impact material behavior. If material behavior for the higher orders displays a similar trend to that of the 1$^{st}$ derivative of deformation, then the emerging material mechanical response could significantly vary. Given the relatively small time-steps for which data is saved by the IFW machine analytics, this process does offer a sensible starting position for these higher derivatives to be analysed, using simplistic differential methods using data at the commencement and end of each recorded time-step. As such, this paper investigates—at a very introductory level—the higher time-derivatives of rotational displacement to understand if these types of fields can be utilized by industry and academia for a more complete understanding of any characteristics drawn out of the process.

## 2. Material and Methods

Ti-6Al-4V hollow axisymmetric cylinders, measuring 80 mm outer diameter, 40 mm inner diameter, 86 mm height, were machined from rolled billet. The as-received Ti-6Al-4V displayed the typical duplex $\alpha/\beta$ microstructure, with globular $\alpha$-phase interspersed by alternating fine laths of $\alpha$ and $\beta$ [8]. The thermal and mechanical fields experienced by the heated (HAZ) and thermo-mechanically affected (TMAZ) regions will cause significant microstructure variations [9].

For each weld, two Ti-6Al-4V cylinders were joined using specialist IFW

equipment. Welding parameters were selected to produce a successful weld (Figure 1), allowing for a comprehensive study of rotational acceleration and higher time-derivatives experienced during manufacture. Two welds were considered, with identical inertial flywheel mass *I*, and forging pressure *P*, but with different initial rotational speeds, thus different stored energies.

## 3. Theory

The stored energy available via the flywheel at the start of an inertia welding process $E_{rot}$, which gets converted to thermal and mechanical energy, is defined in Equation (1), whereby $I$ is flywheel inertial mass, and $\omega$ is initial rotation speed, in rad·s$^{-1}$.

$$E_{rot} = 0.5 \cdot I\omega^2 \tag{1}$$

Two inertia welded samples were analysed, with a "high" stored energy and a "low" stored energy, as result of a high and low initial rotational velocity. The inertial mass of the flywheel was held constant, and initial rotational velocities of 185 rad·s$^{-1}$ and 150 rad·s$^{-1}$ respectively were employed. Due to the square of the rotational velocity term in the energy equation (Equation (1)), this corresponds to $1.5E$ and $E$ as initial stored energies.

In order to calculate the rotational acceleration and higher derivatives, some simplifications were applied to the rotational velocity data. As instantaneous calculations of these terms, particularly the higher derivative terms, may get very high, so the data was discretised to consider 0.05 s intervals, and the time-derivatives of the rotational position were calculated as follows, whereby $\theta$ is rotational position, and so rotational velocity $\omega(t) = \mathrm{d}\theta/\mathrm{d}t$.

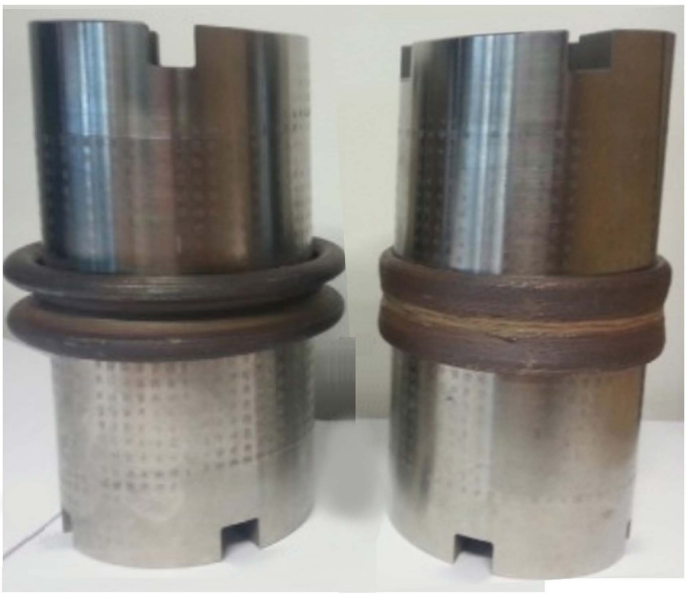

(a) (b)

**Figure 1.** Inertia friction welded Ti-6Al-4V coupons.

$$\text{rotational acceleration } (\text{rad}\cdot\text{s}^{-2});\ \alpha^{\rightarrow}(t) = \mathrm{d}\omega/\mathrm{d}t \equiv f\left\{\left(\mathrm{d}^2\theta\right)/\left(\mathrm{d}t^2\right)\right\} \quad (2)$$

$$\text{rotational jerk } (\text{rad}\cdot\text{s}^{-3});\ \zeta^{\rightarrow}(t) = \mathrm{d}\alpha/\mathrm{d}t \equiv f\left\{\left(\mathrm{d}^3\theta\right)/\left(\mathrm{d}t^3\right)\right\} \quad (3)$$

$$\text{rotational jounce or snap } (\text{rad}\cdot\text{s}^{-4});\ s^{\rightarrow}(t) = \mathrm{d}\zeta/\mathrm{d}t \equiv f\left\{\left(\mathrm{d}^4\theta\right)/\left(\mathrm{d}t^4\right)\right\} \quad (4)$$

$$\text{rotational crackle } (\text{rad}\cdot\text{s}^{-5});\ c^{\rightarrow}(t) = \mathrm{d}s/\mathrm{d}t \equiv f\left\{\left(\mathrm{d}^5\theta\right)/\left(\mathrm{d}t^5\right)\right\} \quad (5)$$

$$\text{rotational pop } (\text{rad}\cdot\text{s}^{-6});\ \varrho^{\rightarrow}(t) = \mathrm{d}c/\mathrm{d}t \equiv f\left\{\left(\mathrm{d}^6\theta\right)/\left(\mathrm{d}t^6\right)\right\} \quad (6)$$

The names snap, crackle and pop are informally used by engineers and scientific community [10] to describe the 4th, 5th, 6th derivatives of position. Given that rotational position has units of radians, so units of the derivative terms in Equation (2) to Equation (6), are of the form rad·s$^{-n}$.

## 4. Results

### 4.1. Rotational Velocity and Acceleration

The rotational velocity curves from the two inertia welds were differentiated multiple times over 0.05 s intervals, to generate the functions for rotational acceleration and higher derivatives. The velocity rundown curve and the rotational acceleration are presented in **Figure 2**. The rundown curves from **Figure 2(a)** are well-considered amongst Inertia welding engineers, and these illustrate the gradual decrease over the process, until the last ~0.5 s, when a rapid drop-off of velocity to zero, indicative of inertia welds, is observed. The rotational acceleration curves are less considered.

Note from the graphs in **Figure 2(b)** that the same trend is observed, whereby after the first 0.2s of rotation, in both welds the deceleration is approximately −60 rad·s$^{-2}$ and this increases toward approximately −30 rad·s$^{-2}$, and then plateaus for the majority of the process, until the final 0.5 s of the weld when it dramatically shoots toward −180 rad·s$^{-2}$, before a sharp change and reducing deceleration toward zero as the stored flywheel energy fully dissipates. Comparing the

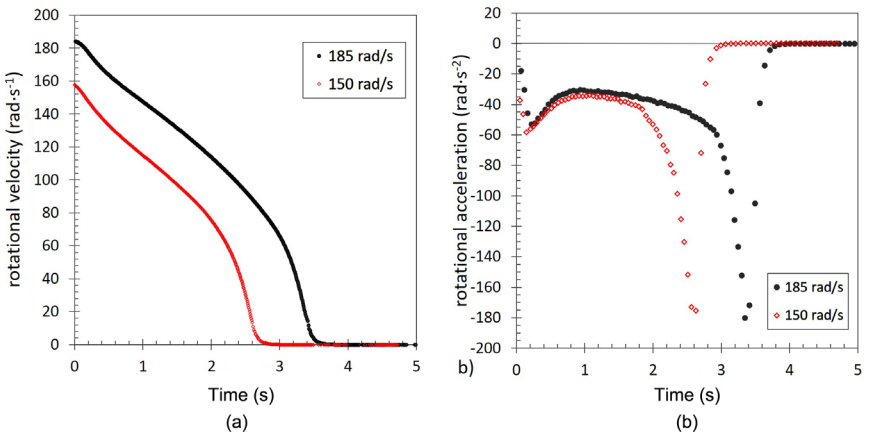


**Figure 2.** (a) rotational velocity versus time curves, and (b) rotational acceleration versus time curves, for the welds.

curves in Figure 2(b) it is interesting to note that the levels of local extrema are surprisingly similar, and the curves mainly differ in the plateau length. This indicates that underlying metallurgical processes governing the initial and final transients, as well as the steady-state regime, are similar across welds. The only difference is the amount of energy available to drive the process, which determines the time-base of the steady-state regime.

### 4.2. Rotational Jerk and Snap

Similarly, the evolution during the process of rotational jerk, Figure 3(a), and rotational jounce, or snap, Figure 3(b), were analysed for trends. Both welds display rotational jerk traces in the first 0.2 s at a very negative value, −200 to −300 rad·s$^{-3}$, although this rapidly rises to a positive jerk, approximately 50 to 60 rad·s$^{-3}$. For both welds these jerk values gradually decrease through the welding process, down through zero and in to negative values toward −50 rad·s$^{-3}$ at approximately 0.5 s before the end of the weld. In the last 0.5 seconds, the rotational jerk spikes to −500 rad·s$^{-3}$ before sharply falling to zero.

### 4.3. Rotational Crackle and Pop

Whilst the data for the rotational jounce, or snap (Figure 3(b)) is much more randomly spread between −1000 and 1000 for both welds during of the process, one trend is evident in both data sets. Over the final 0.5 s of welding for each weld, the rotational snap falls to its greatest negative value, approximately −2500 rad·s$^{-4}$, and tends back to zero sharply during the last 0.5 s. As with rotational acceleration (Figure 2(b)), the main difference in Figure 3(a) and Figure 3(b) is the time-base of the steady-state regime.

Finally, the highest order time-derivatives of position, the informally-named crackle and pop terms, were analysed. Time-bases were reduced to 0.1 s for these terms, to reduce the considerable noise in the differentials. The rotational crackle is presented in Figure 4(a), and the rotational pop in Figure 4(b). Notice a

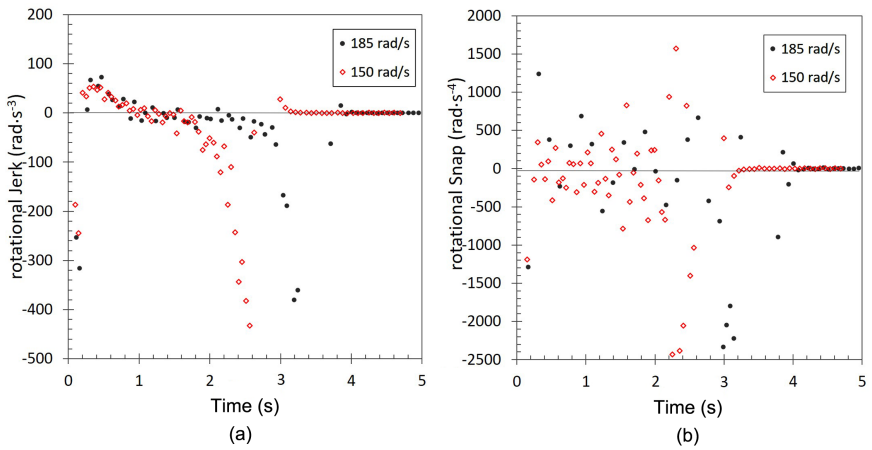


Figure 3. (a) Rotational jerk versus time curves, and (b) rotational jounce (or snap) versus time curves, for the welds.

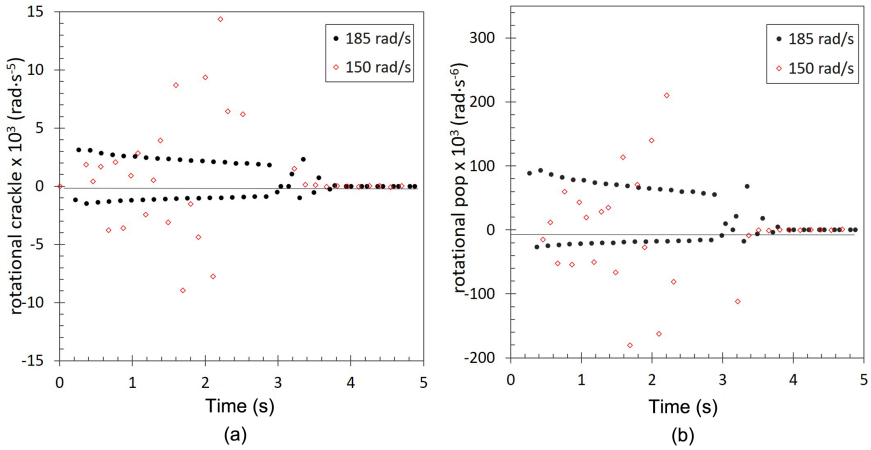


**Figure 4.** (a) Rotational crackle versus time curves, and (b) rotational pop (or snap) versus time curves, for the welds.

distinct oscillatory pattern in the crackle and pop data for the weld commencing at 185 rad·s$^{-1}$. The weld commencing at 150 rad·s$^{-1}$ has been similarly analysed, although noise in the data has made both the crackle and the pop difficult to determine any trend.

One evident feature across both welds is how dynamic the process is, naturally undergoing constant changes throughout. Trends from the acceleration and jerk curves are possibly more intuitive; however the emerging oscillatory trends that appear evident in the highest derivatives are surprising, especially given the more scattered data sets for the rotational snap. For both welds examined it is proposed that initially there was sufficient stored energy to allow the process to form a dynamic steady state. Toward the end of the process the energy remaining ceases to be sufficient to maintain the dynamic steady-state condition. Thus, during the last fraction of a second, similar process phenomena occur within both welds, giving rise to signature trends within the derivative curves, albeit at different times.

It is interesting to observe how the different weld phases show distinctively different sections within each transient curve, in particular the acceleration and the jerk curves. The findings provoke further questions surrounding the process. How would the higher derivative curves appear for poorly chosen welding parameters, which produce poor welds? How would the curves look for a different material? These uncertainties would require further investigation and further experimentation, and are not considered here. However, the derivative study approach overall does potentially open up a greater opportunity for refined process control.

## 5. Conclusions

A study of the time-derivatives, up to the sixth derivative, of rotational position, has been studied for two Ti-6Al-4V inertia friction welds. After a systematic analysis of these results, the following conclusions are drawn.

- Rotational acceleration and jerk traces both display clear patterns across the two welds in terms of behavior of these fields, as the part rotates under action from the flywheel. The rotational snap also displays a pattern in this derivative during the final approximately 0.5s of welding, as the energy dissipates.
- Evidence of a distinct oscillatory pattern in the rotational crackle and pop terms was noted for one weld when differentiating over a larger time-base, though could not be replicated in the 2nd weld, which had no noticeable pattern.
- Higher derivative curves allow distinction of different process regimes, indicating that inertial energy mostly influences the time-base of dynamically steady-state phase. Qualitative differences between initial energies are evident in higher derivatives.
- This novel approach may offer inertia weld specialists, and aerospace engineers who utilize the method, insights toward improving process control, understanding physical phenomena, or cross-comparisons of welds.

## Acknowledgements

We send many thanks to colleagues at the School of Metallurgy and Materials, at the University of Birmingham, with whom discussions were held, which has held to shape this exploratory research.

## Conflicts of Interest

The authors declare no conflicts of interest regarding the publication of this paper.

## References

[1] Li, W., Vairis, A., Preuss, M. and Ma, T. (2016) Linear and Rotary Friction Welding Review. *International Materials Reviews*, **61**, 71-100. https://doi.org/10.1080/09506608.2015.1109214

[2] Attallah, M.M. and Preuss, M. (2012) Chapter 2: Inertia Friction Welding (IFW) for Aerospace Applications. In: Chaturvedi, M.C., Ed., *Welding and Joining of Aerospace Materials*, 2nd Edition, Woodhead Publishing, Cambridge, UK. https://doi.org/10.1016/B978-0-12-819140-8.00002-X

[3] Kallee, S. and Nicholas, D. (1999) Friction and Forge Welding Processes for the Automotive Industry. SAE. https://doi.org/10.4271/1999-01-3214

[4] Nu, H.T.M, Le, T.T., Minh, L.P. and Loc, N.H. (2019) A Study on Rotary Friction Welding of Titanium Alloy (Ti6Al4V). *Advances in Materials Science and Engineering*, **2019**, Article ID 4728213. https://doi.org/10.1155/2019/4728213

[5] Turner, R., Howe, D., Thota, B., Ward. R.M., Basoalto, H.C. and Brooks, J.W. (2016) Calculating the Energy Required to Undergo the Conditioning Phase of a Titanium Alloy Inertia Friction Weld. *Journal of Manufacturing Processes*, **24**, 186-194. https://doi.org/10.1016/j.jmapro.2016.09.008

[6] Wang, L., Preuss, M., Withers, P.J., Baxter, G. and Wilson, P. (2005) Energy-Input-Based Finite-Element Process Modeling of Inertia Welding. *Metallurgical and Materials Transactions B*, **36**, 513-523. https://doi.org/10.1007/s11663-005-0043-y

[7] Lee, M.-S., Hyun, Y.-T. and Jun, T.-S. (2019) Global and Local Strain Rate Sensitiv-

ity of Commercially Pure Titanium. *Journal of Alloys and Compounds*, **803**, 711-720. https://doi.org/10.1016/j.jallcom.2019.06.319

[8] Turner, R.P., Perumal, B., Lu, Y., Ward, R.M., Basoalto, H.C. and Brooks, J.W. (2019) Modeling of the Heat-Affected and Thermomechanically Affected Zones in a Ti-6Al-4V Inertia Friction Weld. *Metallurgical and Materials Transactions B*, **50**, 1000-1011. https://doi.org/10.1007/s11663-018-1489-z

[9] Ji, Y., Wu, S. and Zhao, D. (2016) Microstructure and Mechanical Properties of Friction Welding Joints with Dissimilar Titanium Alloys. *Metals*, **6**, 108-119. https://doi.org/10.3390/met6050108

[10] Visser, M. (2004) Jerk, Snap and the Cosmological Equation of State. *Classical and Quantum Gravity*, **21**, 2603-2616. https://arxiv.org/abs/gr-qc/0309109 https://doi.org/10.1088/0264-9381/21/11/006